



# Brillouin scattering for refractive index sensing in non-adiabatic tapers

E. CATALANO,<sup>1</sup> R. VALLIFUOCO,<sup>1</sup>  R. BERNINI,<sup>2</sup>  L. ZENI,<sup>1</sup> AND A. MINARDO<sup>1,\*</sup> 

<sup>1</sup>Department of Engineering, Università della Campania Luigi Vanvitelli, Via Roma 29, 81031 Aversa, Italy

<sup>2</sup>Istituto per il Rilevamento Elettromagnetico dell'Ambiente, CNR, Via Diocleziano 328, 81024 Napoli, Italy

\*Aldo.Minardo@unicampania.it

**Abstract:** We demonstrate the use of non-adiabatic tapers for refractive index sensing in optical fibers based on Brillouin scattering. By exciting higher order optical modes along the taper, the Brillouin gain spectrum becomes multi-peaked, where each peak exhibits a different sensitivity to the refractive index of the surrounding medium. By this method, we demonstrate a sensitivity enhancement of the Brillouin frequency shift to refractive index changes by a factor of  $\approx 4$ , compared to an adiabatic taper with the same waist diameter. Furthermore, the use of the spectral difference between two Brillouin gain peaks provides a temperature-independent measurement of the external refractive index.

© 2022 Optica Publishing Group under the terms of the [Optica Open Access Publishing Agreement](#)

## 1. Introduction

In the last years, there has been a growing interest in distributed optical fiber sensors. Besides conventional quantities (strain and temperature), new functionalities can be added to these sensors, by making them capable of detecting non-mechanical quantities, such as magnetic field [1] and refractive index [2]. In the latter case, the structure of the fiber is modified to make it locally sensitive to the external refractive index (and absorption) of the outer medium. Furthermore, the adoption of sensing methods based on either Rayleigh scattering [2] or Brillouin scattering [3–5] provides quasi-distributed refractive index sensing capabilities. The taper structure is especially efficient as it allows the interaction of the evanescent optical field with the external medium across the whole fiber circumference. Usually, great care is paid to design adiabatic tapers, where only the local first-order mode of the fiber propagates through the taper, while undergoing relatively little mode conversion to higher-order modes or radiation modes. This condition ensures the realization of tapers with very low insertion loss, which is particularly relevant when several tapers must be realized along the fiber [4]. Nonetheless, the excitation of higher-order modes can be beneficial in some cases. For example, it has been recently demonstrated that the use of multiple optical modes permits the discrimination between temperature and strain effects in Brillouin sensors based on few-mode fibers [6]. Furthermore, higher-order optical modes have a higher sensitivity to the external refractive index, owing to their deeper penetration into the external medium [7].

In this paper, we demonstrate the use of non-adiabatic tapers for refractive index sensing based on stimulated Brillouin scattering (SBS). We show that, the excitation of higher-order modes leads to the formation of a multi-peaked Brillouin gain spectrum (BGS), where each resonant peak is attributed to a specific pump-probe modal pair. Using a resonant peak associated to a higher-order optical mode, a higher sensitivity of the Brillouin frequency shift (BFS) to the external refractive index is obtained. Furthermore, tracking the BFS changes induced by temperature and/or outer refractive index on two distinct resonances, we demonstrate that these two parameters can be determined individually. In particular, we show that the spectral separation provides a self-temperature-compensated measurement of the outer refractive index.

## 2. Characterization of the BFS in non-adiabatic tapered optical fibers

The Brillouin frequency shift (BFS) in optical fibers can be expressed as:

$$BFS = \frac{(n_{eff,pump} + n_{eff,probe})V_a}{\lambda}, \quad (1)$$

where  $n_{eff,pump}$  and  $n_{eff,probe}$  are the effective refractive indexes (ERI) of the pump and probe beams involved in the scattering process,  $V_a$  is the velocity of the acoustic mode, and  $\lambda$  is the optical wavelength. Equation (1) is valid for both intramodal ( $n_{eff,pump} \approx n_{eff,probe}$ ), and intermodal scattering ( $n_{eff,pump} \neq n_{eff,probe}$ ), i.e. when the interacting beams are guided in distinct spatial modes. In single-mode fibers, only intramodal scattering can occur, therefore a multi-peaked BGS may only arise due to the presence of multiple acoustic modes [8]. Vice versa, in multimode optical fibers each pump-probe modal pair generally leads to distinct resonances, also depending on the number of involved acoustic modes [6,9]. When a single-mode optical fiber is tapered, the change of its cross-section leads to modifications in both the ERI and effective acoustic velocity [4]. Specifically, when the core diameter is reduced below the optical wavelength, the light can no longer be confined into the core, thus it reaches the cladding diameter and reflects at the cladding/air interface. Consequently, the tapered fiber becomes multimodal due to the large refractive index contrast between the cladding and the air. In Ref. [4] we have shown that, in an adiabatic taper, the BGS exhibits a single, well-defined Brillouin gain peak related to the interaction of the fundamental optical mode (LP<sub>01</sub>) of the pump and probe fields, and the fundamental longitudinal acoustic mode (L01). In that case, the transition region of the taper was designed to satisfy the adiabaticity criterion [10]. In brief, the local taper angle along each transition region was set to be a fraction  $f$  (with  $f < 1$ ) of the critical angle  $\Omega(z) = (\rho/2\pi) \times (\beta_1 - \beta_2)$ , where  $\rho(z)$  is the core radius, while  $\beta_1$  and  $\beta_2$  are the local propagation constants of the LP<sub>01</sub> and LP<sub>02</sub> modes, respectively. Now, let us suppose that the adiabaticity criterion is not satisfied, i.e., the taper transitions are sufficiently steep to lead to the excitation of high-order optical modes into its waist. Due to radial symmetry, we can safely assume that only the radially symmetric optical modes (LP<sub>0x</sub>) are excited into the taper. Furthermore, for a taper diameter equal to several times the optical wavelength, as the one considered here (10  $\mu\text{m}$ ), the Brillouin scattering is dominated by L-acoustic quasi-plane waves [11], i.e., shear acoustic waves can be safely neglected. We further suppose that coupling primarily occurs between the fundamental optical mode of the untapered fiber, and the first two optical modes of the taper waveguide (LP<sub>01</sub> and LP<sub>02</sub>). Denoting with  $k_1$  the power coupling factor for the LP<sub>01</sub> mode, and with  $P_{P0}$  the power of the pump beam injected into the fiber, the power of the pump beam guided into the LP<sub>01</sub> mode of the taper will be  $k_1 P_{P0}$  (see Fig. 1). Similarly, the power of the probe wave guided into the LP<sub>01</sub> mode of the taper will be  $k_1 P_{S0}$ , where  $P_{S0}$  is the power of the probe beam injected into the fiber from the opposite side (we assume that the two transition regions of the taper are perfectly identical). The gain of the SBS interaction between these two modes will be proportional to  $k_1^2 P_{P0} P_{S0} G_{01}$ , where  $G_{01}$  is a factor depending on the spatial overlap between the interacting optical and acoustic fields [8].

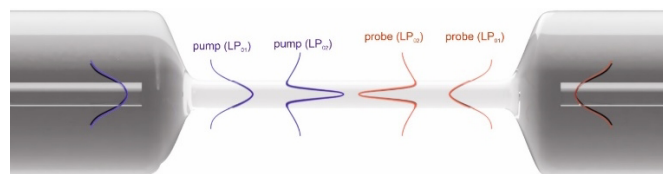


**Fig. 1.** Interaction between pump and probe beams in a non-adiabatic taper.

As the probe gain is observed after transmission along the taper, this factor must be further multiplied by  $k_1$ , due to transmission through the downtaper region. This finally leads to an efficiency factor equal to  $k_1^3 P_{P0} P_{S0} G_{01}$ . Following a similar reasoning, the probe gain associated to the LP<sub>02</sub>-LP<sub>02</sub> interaction, as observed at the receiver, will be proportional to  $k_2^3 P_{P0} P_{S0} G_{02}$ , where  $k_2$  is the fraction of power coupled to the LP<sub>02</sub> mode of the taper for both pump and probe waves, while  $G_{02}$  is the corresponding acousto-optic overlap coefficient. Besides intramodal scattering, intermodal scattering should be considered as well. In our taper, we have two possible interactions: the one between the LP<sub>02</sub> mode of the pump and the LP<sub>01</sub> mode of the probe, and the one between the LP<sub>01</sub> mode of the pump and the LP<sub>02</sub> mode of the probe. It is easy to verify that the former will give rise to a probe gain, at the receiver side, proportional to  $k_1^2 k_2 P_{P0} P_{S0} G_{0102}$ , while the latter will produce a probe gain equal to  $k_1 k_2^2 P_{P0} P_{S0} G_{0102}$ . In both cases, the coefficient  $G_{0102}$  is dependent on the spatial overlap between the LP<sub>01</sub>-LP<sub>02</sub> optical mode pair, and the involved acoustic mode. As in the case of intramodal scattering, we suppose that only one acoustic mode comes into play. In fact, for a nominal diameter of the waist of 10  $\mu\text{m}$ , as the one considered in this paper, we have verified through numerical simulations that both intermodal and intramodal scattering involving the optical modes LP<sub>01</sub> and LP<sub>02</sub>, are mostly efficient when the interaction occurs through the fundamental acoustic mode L01. The relative amplitudes of the Brillouin peaks can be estimated by taking the ratio between the previously estimated factors. Denoting with  $k = k_1/k_2$  the ratio between the coupling coefficients, and assuming  $G_{01} \approx G_{02} \approx G_{0102}$  [12], it is deduced that the Brillouin gain peak due to the LP<sub>01</sub>-LP<sub>01</sub> intramodal scattering will be  $\sim k$  times larger than the peak due to the LP<sub>02</sub> component of the pump and the LP<sub>01</sub> component of the probe,  $\sim k^2$  times larger than the one due to the LP<sub>01</sub> component of the pump and the LP<sub>02</sub> component of the probe, and  $\sim k^3$  larger than the one due to the LP<sub>02</sub>-LP<sub>02</sub> intramodal scattering.

For quasi-adiabatic tapers we can assume  $k > 1$ , therefore the dominant peak in the acquired BGS will be due to the LP<sub>01</sub>-LP<sub>01</sub> intramodal scattering, while the other peaks will be progressively smaller. We note that, the two SBS intermodal mechanisms, while being observed, in general, with a different efficiency, will result in a Brillouin gain peak centered at the same pump-probe frequency detuning (see Eq. (1)).

### 3. Experimental results

In the following, we report the experimental characterization of the Brillouin scattering in two different tapers. The two tapers have the same nominal waist length (20 mm) and diameter (10  $\mu\text{m}$ ), while they differ in the length of the transition region, being 15 mm for the first taper, and 1 mm for the second one. Therefore, the total length of the first taper is 50 mm, while being 22 mm for the second taper. The normalized profiles of the transition regions in both tapers are shown in the inset of Fig. 2. Using the adiabatic criterion discussed earlier, we have verified that a transition length of 15 mm is sufficient to ensure an adiabatic transition, while a transition length of 1 mm is not. Both tapers were realized in a standard SMF-28 optical fiber, using a Vytran GPX-3800 glass fiber processing system [4].

The system makes use of a filament furnace to heat the fiber to its softening point, while applying a tensile force to elongate the fiber and then reduce its cross section. The Vytran GPX-3800 ensures a good reproducibility and a precise control of the geometry of the fabricated tapers, provided that relatively fresh filaments are employed and that these filaments are subjected to a proper normalization procedure before each use. In order to experimentally verify the excitation of higher-order modes, the transmission spectrum of each taper was acquired by launching on it the light from a broadband source (EXFO FLS-2200) and monitoring the transmitted light by an optical spectrum analyzer (HP 86142A). The results for the two tapers are shown in Fig. 2. As expected, the spectra reveal that the first taper is adiabatic, while some modal interference occurs in the shorter taper. For the latter, the measured fringe contrast (FC) is  $\approx 4.2$  dB. From

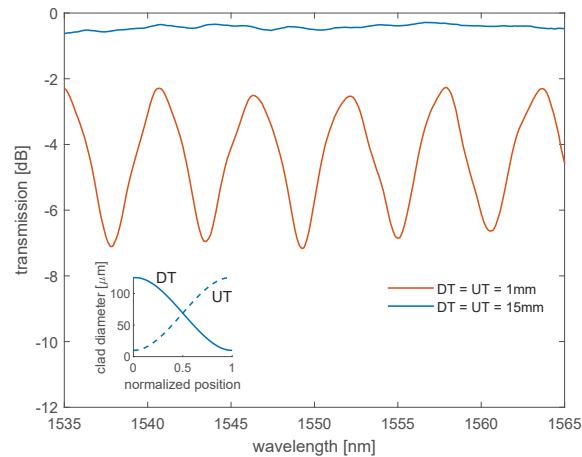


**Fig. 2.** Transmitted spectrum of the fabricated tapers. The inset shows the downtaper (DT) and uptaper (UT) profiles of the fabricated tapers as a function of the position, with the latter normalized to the length of the transition region.

this value, one can derive the ratio  $k = k_1/k_2$  between the intensities of the two interfering beams. In fact,  $FC = -10\log_{10}(1 - V)$ , while the visibility  $V = 2k/(1 + k^2)$  [13]. Note that, in the visibility expression we have considered that the taper contains two transition regions. Using the experimentally determined FC, and assuming  $k > 1$ , we derive  $k \approx 2.9$ . Therefore, while the BGS of the first taper is expected to exhibit only one resonance peak associated to the LP01 intramodal scattering [4], the BGS of the second taper should be composed by at least two peaks, due to the co-presence of intramodal and intermodal SBS scattering. We further observe that the transmission spectrum of the non-adiabatic taper shows a free spectral range (FSR) of  $\approx 5.6$  nm. From the measured FSR, we estimate a difference  $\Delta n$  between the ERI of the interacting beams equal to  $\lambda^2/(FSR \times L) \approx 2.15 \times 10^{-2}$  (we set  $L = 20$  mm). This is in fair agreement with the difference between the ERI of the first two modes, as calculated for a 10- $\mu\text{m}$  taper using the finite-element-method (FEM) solver Comsol Multiphysics, and equal to  $1.96 \times 10^{-2}$  (for the simulation, we used  $n_{core} = 1.452$ ,  $n_{clad} = 1.448$ , and a core radius of the untapered fiber  $r_{core} = 4 \mu\text{m}$ ). The discrepancy between numerical and experimental values is mostly attributed to the diameter of the taper, which is only approximately equal to the nominal value set on the Vytran glass processor. We also note that, the maximum transmission loss of the first taper is  $\approx 0.5$  dB, while that of the second taper is  $\approx 7$  dB. While in SBS measurements the optical loss can be minimized by tuning the laser wavelength to one of the taper transmission maxima, the inherently higher loss of non-adiabatic tapers limits their number along the same fiber to only a few.

As a next step, the BGS of the two tapers were measured using a high spatial resolution Brillouin optical frequency domain analyzer (BOFDA). Details about the system can be found in Ref. [4]. In brief, the setup makes use of a single laser source, emitting at 1550 nm, to provide both the pump and probe lights through double sideband modulation. The pump light is modulated by means of an electro-optic modulator driven by the output port of a vector network analyzer (VNA). Due to Brillouin scattering, the counterpropagating probe light acquires an intensity modulation at the same frequency, which is retrieved, in amplitude and phase, by the VNA. The VNA scan is performed several times, while varying the detuning between the pump and probe frequencies. In all measurements shown below, the VNA frequency was swept from 2 MHz to 12.8 GHz, ensuring a spatial resolution of 8 mm [14]. In Fig. 3 we compare the BGS measured at the middle position of the two realized tapers. The BGS of the adiabatic taper

exhibits only one relevant peak, centered at 11,104 MHz and with a bandwidth of 34 MHz. These data are consistent with those reported in Ref. [4] for adiabatic tapers. More remarkably, the BGS of the non-adiabatic taper exhibits two relevant peaks, the dominant one being centered at 11,130 MHz and with a bandwidth of 29 MHz, and a minor one centered at 11,032 MHz and with a bandwidth of 40 MHz. Based on our theoretical considerations, this minor peak is attributed to the intermodal scattering induced by the  $LP_{02}$  mode of the pump wave, interacting with the  $LP_{01}$  mode of the probe wave. Using, as acoustic velocity, the one calculated by COMSOL for the first acoustic mode,  $V_{a01} = 5950 \frac{m}{s}$ , (we used the parameters reported in Ref. [7] for this calculation), the resulting spectral distance between the two peaks visible in the BGS of the non-adiabatic spectrum should be  $(\Delta n \times V_{a01})/\lambda = 75 \text{ MHz}$ . While this frequency is lower than the observed one (i.e., 98 MHz), we should consider that the ERI of the  $LP_{01}$  and  $LP_{02}$  modes are strongly related to the taper diameter, which may differ from its nominal value due to fabrication tolerance. For example, for a taper diameter of  $9 \mu\text{m}$ , the difference between the ERI of the  $LP_{01}$  and  $LP_{02}$  modes, as calculated by COMSOL, becomes  $2.41 \times 10^{-2}$ , resulting in a spectral distance between the two Brillouin peaks of 92 MHz, which is much closer to the experimental value. Finally, we observe that the difference of  $\sim 26 \text{ MHz}$  between the BFS of the dominant peak in the two spectra shown in Fig. 1, can be attributed to some residual stress deriving from the tapering process. It is also interesting to observe that, the main peak is about 2.3 times higher than the secondary peak, which is in fair agreement with the intensity ratio  $k$  determined from the transmission spectrum ( $k = 2.9$ ). The remaining discrepancy can be attributed to the difference between the strengths of the optomechanical coupling gain for intramodal and intermodal scattering. Based on our simulations, in fact, the intermodal scattering coefficient  $G_{0102}$  was  $\approx 83\% G_{01}$ , resulting in a corrected intensity ratio equal to  $k \frac{G_{01}}{G_{0102}} \approx 2.4$ , in quite close agreement with the experimental value.

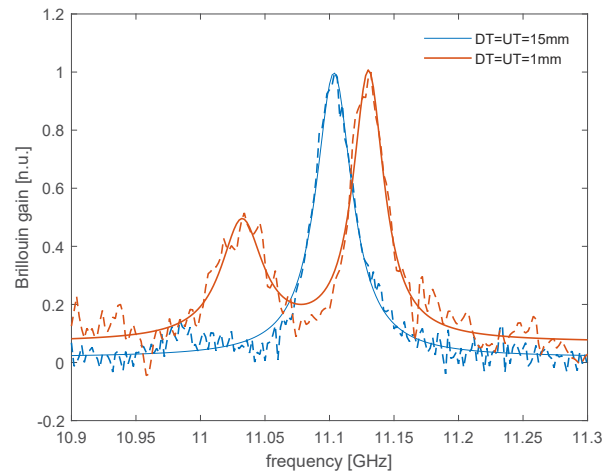


**Fig. 3.** Brillouin gain spectrum measured along tapers with different transition regions. Dashed lines are experimental data, while solid lines represent the Lorentzian fits.

Based on our theoretical analysis, a third peak should appear in the measured BGS due to the  $LP_{02}$  intramodal scattering, downshifted by the main peak by twice the shift from the second peak. However, this peak is  $k^3$  times smaller than the main peak. For  $k = 2.9$ , this corresponds to an imbalance factor of  $\approx 24$ . Furthermore, our simulations indicate that the intramodal scattering coefficient  $G_{02}$  was  $\approx 66\% G_{01}$ , resulting in a corrected intensity ratio equal to  $k^3 \frac{G_{01}}{G_{02}} \approx 37$ . Unfortunately, the signal-to-noise ratio of our measurements was not sufficiently high to distinguish this peak from noise.

As a next step, we have analyzed the variation of the BFS in the two tapers, upon immersion into liquids with different refractive indexes. The liquids were water/glycerin solutions at different concentrations. As regards the first, adiabatic taper, the BFS has been observed to shift with the refractive index following the same behavior reported in Ref. [4], therefore the results are not repeated here for brevity. As regards the second, non-adiabatic taper, a different sensitivity to refractive index was observed for the two resonances. As an example, we report in Fig. 4 the BGS measured with the taper surrounded by air, or water ( $n_{ext} = 1.33$ ), together with the corresponding Lorentzian fits. The figure clearly reveals that, while the shift of the main peak is barely noticeable, the secondary peak (i.e., the one due to intermodal scattering), shifts by about 14 MHz. This agrees with the fact that the secondary peak is influenced by the ERI of both LP<sub>01</sub> and LP<sub>02</sub> modes, while the main peak is solely influenced by the ERI of the LP<sub>01</sub> mode.

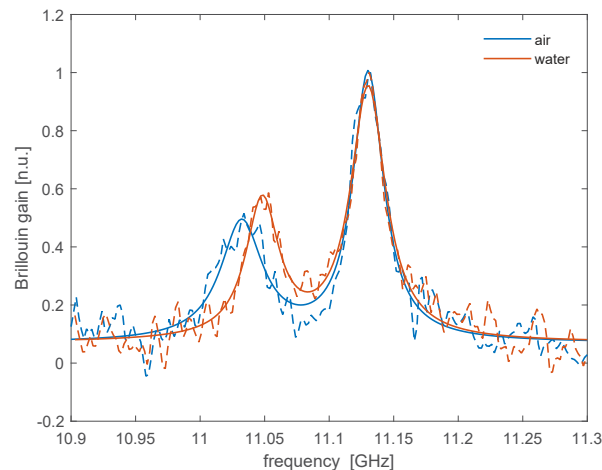


**Fig. 4.** Brillouin gain spectrum measured along the non-adiabatic taper, with the taper surrounded by air or water. Dashed lines are experimental data, while solid lines represent the Lorentzian fits.

Other measurements were then performed, by varying the refractive index of the surrounding medium up to 1.42. The taper was rinsed off using deionized water at the end of each refractive index measurement. We report in Fig. 5 the variation of the BFS of the two Brillouin peaks, as a function of the external refractive index. The experimental values are compared to numerical values, obtained by using COMSOL to determine the ERI of the optical modes in the taper with a waist diameter of 9  $\mu\text{m}$ , and Eq. (1) to derive the corresponding BFS changes (we still assume  $V_{a01} = 5950 \frac{m}{s}$ ). In line with our expectations, the BFS associated to intermodal scattering is more sensitive to the outer refractive index. In fact, the sensitivity of the peak associated to intermodal scattering is about 340 MHz/RIU at  $n_{ext} = 1.39$ , while the one related to intramodal scattering is the same as the one observed in the adiabatic taper ( $\approx 90$  MHz/RIU at  $n_{ext} = 1.39$ ) [4]. Note that, the BFS related to the intermodal scattering is reported only up to an outer refractive index of 1.39. In fact, for  $n_{ext} = 1.42$ , the corresponding peak was too weak to permit an acceptable estimate of the BFS. This can be attributed to the fact that, when the outer refractive index approaches the refractive index of the silica cladding, the LP<sub>02</sub> mode field extends too deeply into the external medium; therefore, the overlap with the acoustic wave is too low to permit an efficient optomechanical interaction.

While the results in Fig. 5 put in evidence that the two resonances respond differently to changes in the outer refractive index, we expect that they shift equally with temperature. Under this hypothesis, the spectral separation between the two Brillouin peaks can be used to obtain a self-temperature-compensated measurement of the outer refractive index. It is important to

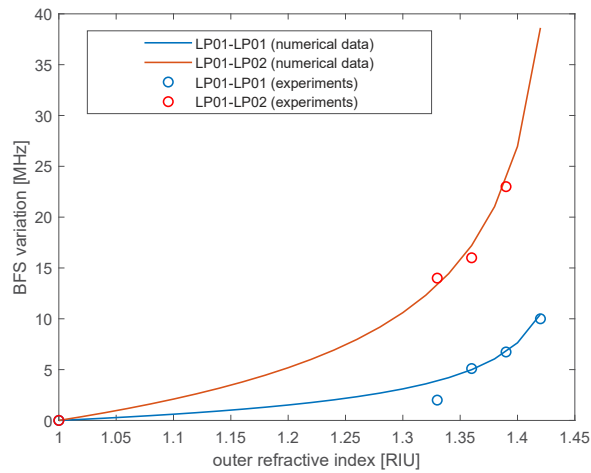


**Fig. 5.** BFS variation as a function of the outer refractive index, for the two Brillouin peaks of the non-adiabatic taper.

observe that, while in Ref. [6] the Brillouin peaks associated to the different spatial modes of a few-mode fiber were reported to exhibit a slightly different temperature sensitivity, such difference was due to variations in the doping concentration across the fiber section. In our case, the tapered fiber can be seen as a uniform silica rod; therefore, no difference between the temperature sensitivity of the different optical modes is expected. In Fig. 6(a), we report the experimentally determined spectral distance between the two Brillouin peaks of the non-adiabatic taper, as a function of the outer refractive index, at a fixed temperature of 20°C. Still, the experimental data are compared to numerical simulations carried out for a taper diameter of 9  $\mu\text{m}$ . Given the tolerance of the fabrication process and the uncertainty in fiber parameters, the experimental results are in satisfactory agreement with our model (the maximum deviation between experimental and numerical data is  $\approx 5.5$  MHz). Figure 6(b) reports the spectral distance between the two Brillouin resonances, as measured upon heating the taper up to 39°C, while keeping the taper surrounded by air or water. For these tests, the taper was heated by hot air in the former case, or by immersing it into hot water in the latter case. The temperature of the taper was retrieved from the BFS of the main resonance, assuming a sensitivity of 1 MHz/°C.

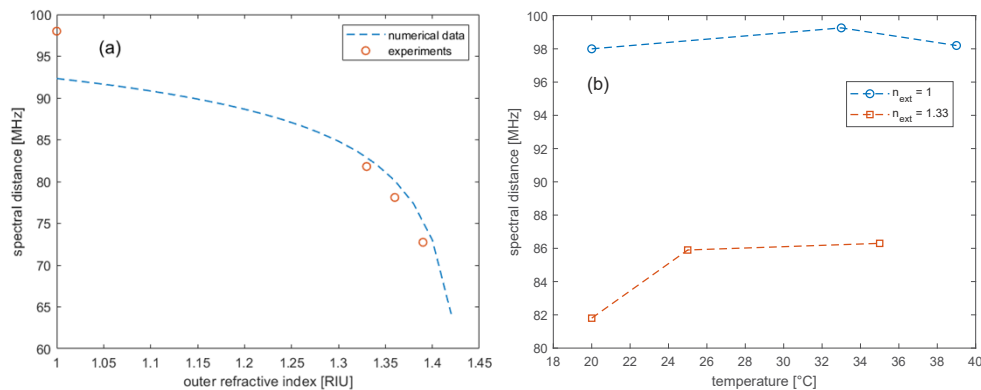


**Fig. 6.** Spectral distance between the two Brillouin peaks of the non-adiabatic taper, as a function of the outer refractive index (a), or temperature (b).

We see that, the spectral distance between the two resonances is relatively stable (within our experimental uncertainty). In particular, the observed variation of the spectral distance between the two Brillouin peaks was less than 1.3 MHz with the taper surrounded by air, or less than 4.5 MHz with the taper surrounded by water. Despite the limited SNR, and the resulting uncertainty in the determination of the position of each Brillouin peak, our analysis confirms that the spectral distance between two Brillouin resonances can be used as a self-temperature-compensated indicator of the outer refractive index.

#### 4. Conclusions

In this paper, we have characterized the Brillouin response of a non-adiabatic taper to changes in the surrounding refractive index. Differently from the adiabatic taper reported in Ref. [4], non-adiabatic tapers exhibit more than one Brillouin resonance, because of the excitation of multiple optical modes in the waist region. The results demonstrate that the excitation of higher-order modes allows to enhance the sensitivity of the BFS to the outer refractive index, without reducing further the waist diameter and therefore weaken the structure. For example, in our experiments we have demonstrated the enhancement of the BFS sensitivity by a factor of  $\approx 4$ . Furthermore, the presence of multiple resonances is helpful in realizing temperature-independent measurements of the external refractive index. We also underline that, while SBS in few-mode fibers has already demonstrated through the selective excitation of each optical mode [12], the experiments reported here show that the Brillouin scattering from more optical modes can be simultaneously excited and detected, by using a taper with a proper design of the transition regions. As a future development, we plan to design a proper package to protect the tapered region, while still ensuring the interaction of light with the external medium for refractive index measurements.

**Funding.** Università degli Studi della Campania Luigi Vanvitelli (Programma "Valere").

**Disclosures.** The authors declare no conflicts of interest.

**Data availability.** Data underlying the results presented in this paper are not publicly available at this time but may be obtained from the authors upon reasonable request.

#### References

1. A. Masoudi and T. P. Newson, "Distributed optical fiber dynamic magnetic field sensor based on magnetostriction," *Appl. Opt.* **53**(13), 2833–2838 (2014).
2. Z. Ding, K. Sun, K. Liu, J. Jiang, and T. Liu, "Distributed refractive index sensing based on tapered fibers in optical frequency domain reflectometry," *Opt. Express* **26**(10), 13042–13054 (2018).
3. C. Huang, H. Sun, H. Liang, L. Cheng, L. Chen, X. Bao, and B. O. Guan, "Refractive index sensing based on Brillouin scattering in a micro fiber," *Appl. Phys. Express* **12**(8), 082013 (2019).
4. E. Catalano, R. Vallifuoco, R. Bernini, L. Zeni, and A. Minardo, "Quasi-distributed refractive index sensing by stimulated Brillouin scattering in tapered optical fibers," *J. Lightwave Technol.* **40**(8), 2619–2624 (2022).
5. R. Bernini, G. Persichetti, E. Catalano, L. Zeni, and A. Minardo, "Refractive index sensing by Brillouin scattering in side-polished optical fibers," *Opt. Lett.* **43**(10), 2280–2283 (2018).
6. A. Li, Y. Wang, J. Fang, M.-J. Li, B. Y. Kim, and W. Shieh, "Few-mode fiber multi-parameter sensor with distributed temperature and strain discrimination," *Opt. Lett.* **40**(7), 1488–1491 (2015).
7. J. Shi, S. Xiao, L. Yi, and M. A. Bi, "A Sensitivity-Enhanced Refractive Index Sensor Using a Single-Mode Thin-Core Fiber Incorporating an Abrupt Taper," *Sensors* **12**(4), 4697–4705 (2012).
8. Y. Koyamada, S. Sato, S. Nakamura, H. Sotobayashi, and W. Chujo, "Simulating and designing Brillouin gain spectrum in single-mode fibers," *J. Lightwave Technol.* **22**(2), 631–639 (2004).
9. A. Minardo, R. Bernini, and L. Zeni, "Experimental and numerical study on stimulated Brillouin scattering in a graded-index multimode fiber," *Opt. Express* **22**(14), 17480–17489 (2014).
10. J. D. Love and W. M. Henry, "Quantifying loss minimisation in singlemode fibre tapers," *Electron. Lett.* **22**(17), 912–914 (1986).
11. P. Dainese, P. S. J. Russell, N. Joly, J. C. Knight, G. S. Wiederhecker, H. L. Fragnito, V. Laude, and A. Khelif, "Stimulated Brillouin scattering from multi-GHz-guided acoustic phonons in nanostructured photonic crystal fibres," *Nat. Phys.* **2**(6), 388–392 (2006).
12. K. Y. Song, Y. H. Kim, and B. Y. Kim, "Intermodal stimulated Brillouin scattering in two-mode fibers," *Opt. Lett.* **38**(11), 1805–1807 (2013).



13. G. Testa, Y. Huang, P. M. Sarro, L. Zeni, and R. Bernini, "High-visibility optofluidic Mach-Zehnder interferometer," *Opt. Lett.* **35**(10), 1584–1586 (2010).
14. R. Bernini, A. Minardo, and L. Zeni, "Distributed sensing at centimeter-scale spatial resolution by BOFDA: Measurements and signal processing," *IEEE Photonics J.* **4**(1), 48–56 (2012).